arXiv:1701.06811v1 [cs.SY] 24 Jan 2017

Socio-technical Smart Grid Optimization via Decentralized Charge Control of Electric Vehicles

Evangelos Pournaras, Seoho Jung, Huiting Zhang, Xingliang Fang and Lloyd Sanders

***Abstract*—Electrical vehicles (EVs) play a key role in the sustainability of the environment as they contribute to the reduction of carbon emissions and the harness of natural resources. However, when the Smart Grid powers the charging of EVs, high energy costs and power peaks challenge system reliability with risks of blackouts. This is especially the case when the Smart Grid has to moderate additional uncertainties such as the penetration of renewable energy resources or energy market dynamics. In addition, social dynamics such as the participation in demand-response programs, discomfort experienced from alternative suggested usage of the EVs and even the fairness in the demand-response among the participating citizens perplex even further the operation and regulation of the Smart Grid. This paper introduces a fully decentralized mechanism for charging control of EVs that regulates three Smart Grid socio-technical aspects: (i) robustness, (ii) discomfort and (iii) fairness. By exclusively using local knowledge, a software agent generates energy demand plans in each EV that encode different charging patterns. Agents interact to make collective decisions of which plan to execute so that power peaks and energy cost are reduced. The impact of improving robustness on discomfort and fairness is empirically shown using real-world data under a varied level of EV participation. The findings are used to project the effect of optimization in a future forecasting scenario with mass adoption of EVs charged from the Smart Grid.**

***Index Terms*—electrical vehicle, Smart Grid, decentralized system, optimization, charging control, planning, scheduling, robustness, discomfort, fairness, diffusion of innovation**

I. Introduction

WITH the unavoidable ramifications of climate change bearing down upon us, the collective zeitgeist is moving towards using renewable resources, and eliminating usage of ubiquitous fossil fuels. Although these notions are wide and varied, one progressive step is the elimination of Internal Combustion Engines (ICEs) for transport via Electric Vehicles (EVs). These vehicles, instead of running off petroleum and diesel, are plugged into the main power grid and charged. Once charged, vehicles have a distance of a few hundred kilometers before needing a recharge. Currently, private EVs predominantly charge at home, but more charging stations are being established.

It is predicted that by 2025, EVs could have approximately 22% of the current vehicle market [1], but without investigating the potential impact this could have on existing power infrastructure, this relatively sudden influx could potentially have disastrous consequences on the reliability of power. To nullify such threats to power stability, many studies have investigated different charging schemes from centralized optimized charging to so-called aggregators that pool together a number of vehicles and optimize their charging regimes under various constraints, e.g. operational levels of grids [2], [3]. The organization of charging can have multiple objectives aside from the stability of the power grid infrastructure. These objectives can be considered as global or local objectives. The foremost of which is spot price savings. This is to charge one's vehicle when the spot price on the grid is the least. This can have the implicit implication of also reducing the load on the grid, if managed appropriately. Studies have also looked into EVs as a means of storing reserve power, for example, to lower the volatility of renewable resource energy production, and provide back-up supply to the grid [4].

Herein this paper proposes a new Vehicle to Grid (V2G) charging paradigm for EVs as a Smart Grid enabler: socio-technical decentralized optimization of EV charging. Although the means of scheduling through decentralization has been looked at before, e.g., [5], this work is based on the EPOS [6] mechanism that finds solutions efficiently for a distributed 0-1 multiple-choice combinatorial optimization problem, which is NP hard. EVs are equipped with software agents that run EPOS, possibly via demand-response programs of utility companies. Agents compute power consumption plans that minimize discomfort originated from scheduling and maximize fairness by design, while collective decision-making contributes to lowering power peaks and energy costs. The socio-technical measurements introduced here are novel with very few related studies [7], [8].

Following up the results of optimization, the future impact of mass EV adoption on the Smart Grid is studied. Namely, the adoption diffusion of EVs and their impact given the current infrastructure is modeled over time. A measure of infrastructure lifetime is proposed given the hypothetical uptake of EPOS app in fractions of the future EV mass.

The main contributions of this paper are as follows:

- A new methodology for a socio-technical Smart Grid optimization via decentralized charge control. The scalable mechanism of EPOS is used for this purpose.
- Understanding how optimization of system-wide objectives, e.g. robustness, affect the user discomfort and the social fairness.
- Understanding market penetration of EVs in the future and how this will affect the existing power infrastructure by using a simplified model of innovation diffusion.

This paper is outlined as follows: The following section

Manuscript received Month Date, Year; revised Month Date, 20XX.

Copyright © 20XX IEEE. Personal use of this material is permitted. However, permission to use this material for any other purposes must be obtained from the IEEE by sending a request to pubs-permissions@ieee.org

Professorship of Computational Social Science, ETH Zurich, Zurich, Switzerland. E-mail: {epournaras,sejung,zhuiting,fangx,,lsanders}@ethz.ch

introduces the decentralized operational planning for EVs. Section III illustrates the decentralized decision-making and optimization process employed. It also defines the measures of robustness, discomfort and fairness. Section IV illustrates the data used for the experimental evaluation and the findings from the results. Finally, Section V concludes this paper and outlines future work.

II. Local Operational Planning

This section illustrates how EVs can locally and autonomously plan their power usage in order to achieve various system-wide objectives such as the improvement of system robustness or the reduction of power costs.

A. An overview

This paper introduces the concept of local operational planning of EVs as the means to meet system-wide objectives of power grids. The motivation here is that if adjustments in power demand can be pre-computed and scheduled, operational uncertainties are minimized and more effective regulatory actions can be applied under several operational scenarios, e.g., failures of power generators, price peaks, weather events influencing the availability of renewable energy resources, etc. Planning is well-established approach in literature [9], [10], [11] and in several related real-world application domains [12], [13], [14], [15].

The proposed technical concept concerns a multi-agent system for decentralized operational planning of EVs. Each EV runs software that can autonomously generates a number of possible operational plans that schedule the power consumption of the vehicle when charging from the power grid. Usually this happens when the EV is parked at home or at work. Each plan may cause a varied level of driver discomfort measured empirically by the likelihood of the plan to be interrupted by, for example, an unintended traveling event. Agents make coordinated selections of a plan to execute in order to collectively improve the robustness of the Smart Grid, while driver discomfort can be measured and self-regulated.

Figure 1 illustrates the concept of plan generation. Agents compute *flexibility windows* within which their vehicle is usually available to charge. In practice, windows usually correspond to times in which the vehicle is parked at home. During these times, it charges or it is fully charged and does not consume battery. In each window, *charging slots* are computed in which a full charging can be performed. The agent ranks the slots from low to high according to the likelihood of vehicle usage computed from historic data. Each plan uses a varied number of slots within which the charging is redistributed.

Each EV model has a certain level of power consumption when it charges. The plans redistribute the power usage as illustrated in Figure 2 for Window 3 that belongs to the states of charge in Figure 1c and 1d. For the illustration, a Nissan model equipped with a 6.6 kW onboard charger is used [16].

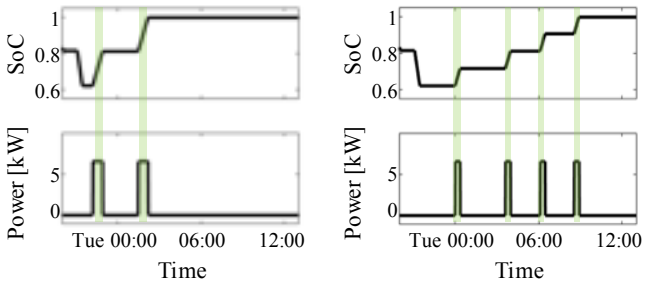

Fig. 2. Power consumption of the Nissan model for Window 3 belonging to the plans of Figure 1c and 1d

B. Technical Concept

This section elaborates on the proposed the technical concept. Assume a number of n EVs powered by a common power system. Each EV is characterized by a model m that determines features such as the battery capacity and charging rate. Production models of EVs are earlier reviewed [17]. Each EV is assumed equipped with an agent i that is a software application controlling the battery charging. Technology for such control is available in the market [18]. The agent is constrained by a minimum time *interval* of size m during which the vehicle can continuously charge without pause.

Each agent i generates a sequence of v plans $D_i = (d_{i,j})_{j=1}^{v}$ that schedule for the future period $T = |d_{i,j}|$ the power consumption of the vehicle when charging from the power grid. These plans may be equivalent for the driver of the vehicle or they may cause different levels of discomfort, for example, each plan may disrupt the regular use of an EV to a different extent. Each agent i selects one and only one plan $d_{i,j} = (d_{i,j,t})_{t=1}^{T}$ to execute according to a selection function $j = f_{\mathsf{s}}(D_i) \in \{1, ..., v\}$ designed to serve a system-wide objective such as the improvement of robustness or the reduction of power cost in the Smart Grid. Robustness concerns how homogeneous the collective power consumption is over time so that power peaks that may cause cascading failures [14], [19] are prevented or mitigated. Cost concerns the monetary value of the collective power consumption governed by the spot price signal $P = (p_t)_{t=1}^{T}$ (USD/kWh) of a power market [20].

Reasoning about plan generation is locally performed based on accumulated historic data that represent a typical temporal pattern usage of the EV and the driver profile, e.g. daily or weekly usage. These data are referred to as $S_i = (s_{i,t})_{t=0}^{T}$, where $s_{i,t} \in [0, 1]$ stands for the state of charge (SoC) of the vehicle at time t. This signal is used as a seed for the plan generation. The goal of plan generation is to compute several ways of charging the EV during times in which the vehicle is not used, e.g., when the vehicle is parked at home. These times are referred to in this paper as the *flexibility windows*, $W_i = (S_{i,w})_{w=1}^{q_i} \subseteq S_i$, of an agent i. Algorithm 1 illustrates how the windows are computed.

The algorithm identifies the times in which the SoC stops decreasing and starts increasing (line 3 of Algorithm 1). These times are the beginnings of the flexibility windows. The end of the windows is detected by the times in which the SoC stops

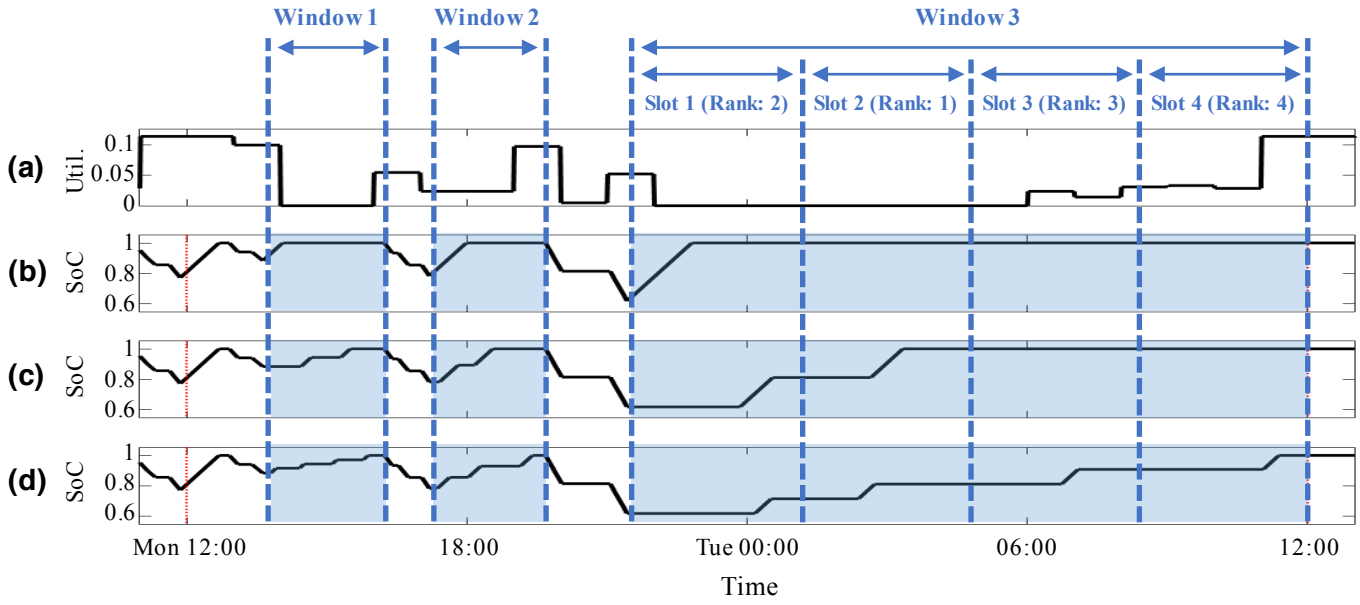

Fig. 1. Plan generation defines flexibility windows within which the SoC increases or does not vary. In each window, severeal charging slots are defined within which a full charging can be performed. Slots are ranked from low to high and according to the likelihood of usage computed from historic data. (a). Likelihood of the vehicle usage derived from historic data. (b). Intended usage of the EV in which charging starts and completes at the very beginning of each window. (c). States of charge in a generated plan that uses Slot 2 and Slot 1 in Window 3. The two slots have the lowest likelihood of usage (d). States of charge in a generated plan that uses all slots in Window 3.

Algorithm 1 Computation of flexibility windows.

Require: S_i

1: w=0;
2: **for** $t = 1$ to T **do**
3: **if** $s_{i,t} < s_{i,t-1}$ **and** $s_{i,t} < s_{i,t+1}$ **then**
4: $w = w + 1$;
5: **while** $s_{i,t} > s_{i,t-1}$ **and** $s_{i,t} \leq s_{i,t+1}$ **and** $t < T$ **do**
6: $S_{i,w} = S_{i,w} \cup s_{i,t}$
7: $t = t + 1$;
8: **end while**
9: **if** $|S_{i,w}| \geq T_{\mathsf{c}}(\mathsf{m}, s_{i,x,w})$ **then**
10: $W_i = W_i \cup S_{i,w}$
11: **else**
12: $w = w - 1$;
13: **end if**
14: **end if**
15: **end for**

Ensure: $W_i, \forall i \in \{1, ..., n\}$

increasing and starts decreasing (line 5 of Algorithm 1). This indicates that the EV is again in use. Figure 3 illustrates how the start and end of a window are detected. The algorithm excludes windows that do not have the length for a full charging[1] (line 9-13 of Algorithm 1). The charging time $T_{\mathsf{c}}(\mathsf{m}, s_{i,t})$ of model m with SoC $s_{i,x,w}$ at the beginning time x of window w is given as follows:

$$l_{i,w} = T_{\mathsf{c}}(\mathsf{m}, s_{i,x,w}) = (1 - s_{i,x,w}) \frac{b_{\mathsf{m}}}{r_{\mathsf{m}}}, \quad (1)$$

[1]The algorithm assumes here that windows of length shorter than the full charging time are more sensitive to user interruptions and therefore have a higher uncertainty when used for scheduling the charging of the vehicle. The evaluation of this assumption with several other algorithm variations is subject of future work.

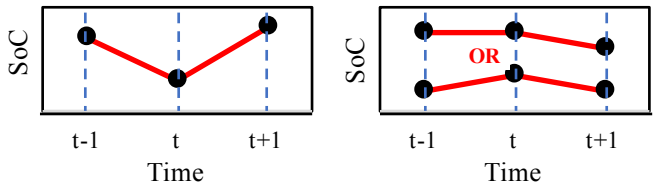

(a) Start of window **(b)** End of window

Fig. 3. Detection of window limits. (a) SoC is lower at $t-1$, and higher at $t+1$. (b) SoC is equal or higher at $t-1$, and lower at $t+1$.

where b_{m} is the battery capacity of model m (kWh) and r_{m} is the charging rate of model m (kW).

The usual operation of an EV suggests that within a window corresponding to 'parked at home' or 'parked at work', the user charges immediately the EV. This action has significant implications. The power consumption mainly occurs at the very beginning of the window instead of at the end. Given that these windows among users have high temporal similarity as they correspond to user behavior and activity, the aggregate energy consumption at the beginning of the windows is synchronized among the EVs and results in power peaks that can potentially cause blackouts or increase the energy cost. Moreover, as the battery technology [21] improves by allowing higher charging rates, the power peaks are expected to become even sharper and more dramatic. This section introduces a model that tackles this limitation by establishing $k_{i,w}$ charging *slots* $Q_{i,w} = (S_{i,w,o})_{o=1}^{k_{i,w}}$ within each window w. The number of slots $k_{i,w} > 0$ is computed by Algorithm 2. Line 2-6 determine the number of slots as follows:

Algorithm 2 Computation of slots number for each window.

Require: W_i, $T_{\mathsf{c}}(\mathsf{m}, s_{i,x,w})$, v
1: **for all** $S_{i,w} \in W_i$ **do**
2: $k_{i,w} = |S_{i,w}|/T_{\mathsf{c}}(\mathsf{m}, s_{i,x,w})$
3: **if** $k_{i,w} \geq v$ **then**
4: $k_{i,w}$=v
5: $l_{i,w} = |S_{i,w}|/k_{i,w}$
6: **end if**
7: $K_i = K_i \cup k_{i,w}$
8: **end for**
Ensure: K_i, $\forall i \in \{1, ..., n\}$

$$k_{i,w} = \begin{cases} |S_{i,w}|/T_{\mathsf{c}}(\mathsf{m}, s_{i,x,w}), & \text{if } k_{i,w} \leq v \\ v, & \text{if } k_{i,w} > v \end{cases}, \tag{2}$$

where $|S_{i,w}|$ is the size of window w, $T_{\mathsf{c}}(\mathsf{m}, s_{i,x,w})$ is the charging time of model m at window w and v determines the maximum number of plans with which an agent can operate. When knowing the number of slots per window, the actual slots can determined according to Algorithm 3.

Algorithm 3 Computation of slots.

Require: W_i, K_i, $l_{i,w}$
1: **for** $w = 1$ to $w = |W_i|$ **do**
2: **for** $o = 1$ to $o = k_{i,w}$ **do**
3: **for** $t = x + o * l_{i,w} - l_{i,w}$ to $x + o * l_{i,w} - 1$ **do**
4: $S_{i,w,o} = S_{i,w,o} \cup s_{i,t,w,o}$
5: **end for**
6: $Q_{i,w} = Q_{i,w} \cup S_{i,w,o}$
7: **end for**
8: **end for**
Ensure: $Q_{i,w}$, $\forall i \in \{1, ..., n\}$ and $\forall w \in \{1, ..., q_i\}$

Plan generation is then performed by redistributing the charging of EVs among the slots. A design choice here is (i) how many slots to use and (ii) which slots to use.

The number of slots determines the extent to redistribution, in other words, how uniform charging is distributed over time. The plans are generated such that the first plan uses one slot, whereas the last plan uses all v slots. Each plan in between uses an additional slot incrementally.

The slots used in each plan are determined by the likelihood of the vehicle usage $U_i = (u_{i,t})_{t=1}^{T}$ extracted from historical data. Based on these data, the slots in each window can be ranked from low to high likelihood of usage. Each plan uses the slots with the lowest usage likelihood so that the likelihood of discomfort is minimized. Therefore, the discomfort g_i of a plan can be defined as follows:

$$g_i = \frac{1}{T} \sum_{t=1}^{T} (1 - s_{i,t}) u_{i,t}, \tag{3}$$

where $s_{i,t}$ is the SoC and $u_{i,t}$ is the likelihood of vehicle usage at time t.

After determining the slots for each plan, charging in each window w is performed in $z_{\mathsf{i}}(\mathsf{m}, s_{i,x,w})$ non-overlapping intervals of m size as follows:

$$z_{\mathsf{i}}(\mathsf{m}, s_{i,x,w}) = \frac{T_{\mathsf{c}}(\mathsf{m}, s_{i,x,w})}{m}, \tag{4}$$

where $T_{\mathsf{c}}(\mathsf{m}, s_{i,x,w})$ is the charging duration and m is the minimum time interval that a vehicle can be charged without pause. The intervals are uniformly distributed across the slots used by each plan. Algorithm 4 illustrates the plan generation process.

Algorithm 4 Computation of agent plans.

Require: S_i, K_i, $Q_{i,w}$, U_i, $l_{i,w}$
1: **for all** $S_{i,w} \in W_i$ **do**
2: $\hat{Q}_{i,w}$=rank($Q_{i,w}$,U_i)
3: **for** $j = 1$ to $j = max(K_i)$ **do**
4: $\hat{S}_i$=shuffle(S_i,j,$\hat{Q}_{i,w}$,$l_{i,w}$,m)
5: $d_{i,j} = d_{i,j} \cup d_{i,j,t}$
6: **end for**
7: **end for**
Ensure: D_i, $\forall i \in \{1, ..., n\}$

The plan generation algorithm iterates over the windows (line 1 of Algorithm 4) and ranks the slots of each window according to the likelihood U_i of vehicle usage (line 2 of Algorithm 4). The window with the maximum number of slots corresponds to the number of plans $v = max(K_i)$ (line 3 of Algorithm 4). Each plan j is generated by randomly shuffling $z_{\mathsf{i}}(\mathsf{m}, s_{i,x,w})$ charging intervals over j slots (line 4 of Algorithm 4). The plan is computed as $d_{i,j} = d_{i,j} \cup d_{i,j,t}$, where:

$$d_{i,j,t} = \begin{cases} e_{\mathsf{m}} > 0, & \text{if } \hat{s}_{i,t} < \hat{s}_{i,t+1} \\ 0, & \text{if } \hat{s}_{i,t} \geq \hat{s}_{i,t+1} \end{cases}, \forall t \in \{1, ..., T-1\} \tag{5}$$

Therefore, each value $d_{i,j,t} \geq 0$ of a plan contain the power consumption e_{m} of model m (kW) at time t for the respective change $\hat{s}_{i,t}$ to $\hat{s}_{i,t+1}$ in SoC.

III. Decentralized Decision-making

Agents employ the EPOS system [6] as a cooperative optimization mechanism for charging EVs in a fully decentralized fashion. EPOS has been studied earlier in demand-response of residential energy consumption [14], [15]. In that scenario, the agents control individual electrical household devices or the aggregate consumption of the household. In contrast, this paper contributes a new application of EPOS to Smart Grids and provides fundamental insights on how the charging of EVs can be modeled as a 0-1 multiple-choice combinatorial optimization problem.

In EPOS, agents are self-organized [22] in a tree topology as a way to structure their interactions with which they perform the cooperative optimization. A tree topology provides a computationally cost-effective aggregation of the power demand level required for coordinating the decision-making. Decision-making is performed bottom-up and level-by-level: children interact with their parent and collectively decide which plan to execute based on (i) their own plans and (ii) the selected plans of the agents connected to each of their branches underneath. Selection is computationally performed by the parent of the children that computes the combinational plans as follows:

$$C_i = (c_{i,j})_{j=1}^{v^k} = \prod_{u=1}^{k} A_u \tag{6}$$

where the parent agent i performs the Cartesian product $\prod_{u=1}^{k} A_u$ to compute all combinations between the sequences of aggregates plans $A_1, ..., A_k$ received by its k children. The child $u = 1$ of agent i is assumed to be the first one and the child $u = k$ the last one. An aggregate plan $a_{u,j} \in A_u$ is computed by summing the plan $d_{u,j}$ and all selected plans of the agents received through the branch underneath child u.

Two selection functions are executed by each parent on behalf of its children and are defined as measures of the Smart Grid robustness: (i) MIN-DEV and MIN-COST. The former aims at minimizing the standard deviation, σ, of the total demand as a measure of load uniformity, load balancing and peak-shaving. The MIN-DEV selection function is defined as follows:

$$j = \arg\min_{j=1}^{v^k} \sigma(c_{i,j}). \tag{7}$$

The MIN-COST selection function aims at reducing the total energy cost by taking into account the temporal energy prices as follows:

$$j = \arg\min_{j=1}^{v^k} \sum_{t=1}^{T} c_{i,j,t} * p_t, \tag{8}$$

where p_t is the energy price at time t.

This paper studies how the technical aspect of robustness may influence human and social aspects such as the discomfort and fairness respectively. The system discomfort G_{d} in the system is measured by the average discomfort as follows:

$$G_{\mathsf{d}} = \frac{1}{n} \sum_{i=1}^{n} g_i. \tag{9}$$

A charging regime is defined as fair if all agents have the same level of discomfort. Fairness increases with the variation of discomfort. Mathematically, it is defined as follows:

$$G_{\mathsf{f}} = 1 - \sigma(g_1, ..., g_n), \tag{10}$$

where $\sigma(g_1, ..., g_n)$ measures the standard deviation of the discomfort values among the agents.

IV. Experimental Evaluation

This section illustrates the dataset used, the results of the decentralized optimization and the future impact of EV mass adoption.

A. Dataset studied

Our experiments are based upon data from the California Department of Transportation's California Household Travel Survey for 2010 – 2012 [23]. This survey carries out multiple objectives in relation to transport with respect to household, person, and vehicle. For our work we focus on the vehicular data, 79011 vehicles. A proportion of the vehicles, 2910, are fitted with GPS: This monitors vehicles continuously for 7 day period (although not the same seven day period for all vehicles) with the resolution of one second (proportions shown in Figure 8).

We use this GPS data, pre-processed by the survey into trip profiles. Essentially, they describe each trip made by the vehicle in question, as a destination (home, work, school, or other), a start/finish trip time, and an average speed. From this data, among other things, we can analyze how vehicles are used on a weekly basis, given their type. From our data pool of 2910 GPS monitored vehicles, we select the EV data which we pool together with the PHEV data to produce an aggregated pseudo-EV data pool of 130 vehicles.[2] Weekly usage of all GPS vehicles in the data set are as shown in Figure 9a.

State of charge and driving profiles: Of interest to us in this data set is how EVs discharge through usage. With this knowledge we can measure the various performance objectives of the model proposed in section II-A. To do this we calculate the EV state of charge (SoC) (percentage of charge remaining in EV batteries). As the SoC is can be used to characterize the use of the vehicle, it is also known as the driving profile. To calculate the SoC, it is deemed sufficient to a first approximation, to assume that when an EV is in transit, it travels at the average speed calculated in the report. In this approximate framework, we assume the power required is proportional to speed, and thus we are able to build a SoC profile for each EV in the data set.[3]

EV efficiency is often given in 'miles per gallon' driven either within the city or on a highway.(For the EV models used in this report, the details are given in Table II – see below for further explanation.) To find the energy consumed (in kWh) during some outing via the fuel efficiency rating, average speed of the vehicle for the duration of the said trip, we use the following formula:

$$E_{\text{trip}} = \frac{d\eta}{f_e}, \tag{11}$$

where $\eta = 33.705$ kWh/gallon (the conversion in energy between gasoline and Joules [25]), $d = s \times t_{\text{trip}}$ is the distance covered in the journey (s the average speed in mph, and t_{trip} the duration of the journey, in hours), and f_e (in miles/gallon) is the fuel efficiency of the vehicle model for a given scenario, either journeying through the city, or on a highway (see Table II). As our vehicular trip data gives an average speed, we select f_e to be that of the city scenario when the average speed is $s \leq 60$ mph, or the highway f_e if $s > 60$mph.

From Eq. (11) we can calculate the energy for every trip taken by a vehicle given its make and model. We can then build up the SoC of the battery as a function of time, knowing its battery capacity, and battery charge rate (Table II).

As the proportionality of power usage is dependent upon the make of the vehicle, we assume that the 130 EVs are split in the same proportion as the current market share of the EVs [26], [27], Table II.

Illustration of the functional form of 3 vehicle SoC profiles from the data are given in Figure 9b.

Caveat: In section II-B, the model espoused relies on historical driver data to understand the probabilistic availability of the vehicle throughout the week; a limitation of the Californian

[2]This balances the trade off of reasonable statistics, with accurate driver profile representation.

[3]Although more advanced models do exist, e.g., [24].

Survey is that the data per vehicle is only a week in length. Therefore, we assume that the data provided by the survey is representative of that vehicle's weekly usage. Although individual vehicles were surveyed at different times, in our calculations we assume that all data is representative and therefore all driving profiles can be amalgamated, and said to be from the same week.

Decentralized Optimization

EPOS is implemented in Protopeer [28] and each experiment is repeated 50 times. Each repetition shuffles the agents randomly in a binary tree topology. All agents generate 4 plans. Four participation scenarios are evaluated. Each scenario assumes that a subset of the EVs is equipped with the capability to generate plans. The rest of the non-participating EVs use the default charging pattern observed in the historic data. The four participation levels are 25%, 50%, 75% and 100%. The planning horizon is set to $T = 1440$ and $T = 10080$ that correspond to daily and weekly optimization respectively.

An overview of the load curves is given in Figure 10. Figure 4 illustrates the performance of EPOS under MIN-DEV and MIN-COST. The performance is measured by the relative to the control data, decrease in standard deviation and cost respectively. The relative deviation reduction under daily optimization is on average 50.3%, 53.0%, 41.0% and 23.2% for 25%, 50%, 75% and 100% participation level. Respectively, the relative reduction under weekly optimization is 49.8%, 51.9%, 39.81% and 22.5%. The relative cost reduction under daily optimization is on average 48.9%, 34.7%, 23.1% and 13.2% for 25%, 50%, 75% and 100% participation level. For weekly optimization, the respective cost reduction is 47.0%, 33.4%, 22.0% and 12.8%.

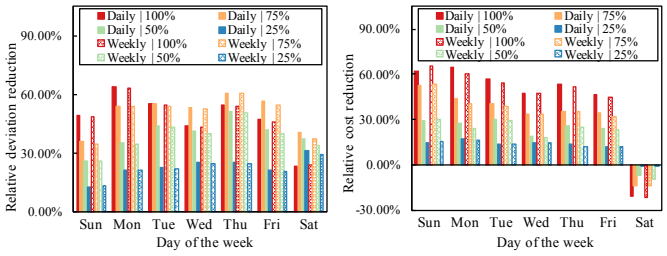

(a) MIN-DEV **(b)** MIN-COST

Fig. 4. Performance of EPOS under varied participation level.

Figure 5 illustrates the probability of plan selections in the performed experiments. The probability of plan selection for daily optimization in MIN-DEV under 100% participation is on average 0.15, 0.12, 0.15 and 0.59 for plan 1 to 4 respectively. In contrast, the respective probabilities for MIN-COST change as follows: 0.20, 0.22, 0.14 and 0.46. The higher number of selections for plan 4 is more significant in MIN-DEV. Moreover, in daily optimization with MIN-DEV the plan with the highest probability is plan 4 (0.55), 4 (0.57), 4 (0.60), and 4 (0.59) for each of the 25%, 50%, 75% and 100% participation levels. The respective plan with the lowest probability is 2 (0.14), 2 (0.13), 2 (0.12), and 2 (0.12).

In weekly optimization, the probability of plan selection in MIN-DEV under 100% participation is on 0.21, 0.17, 0.23 and 0.38 for plan 1 to 4 respectively. The respective probabilities change dramatically in MIN-COST: 0.57, 0.30, 0.07 and 0.06. In addition, under MIN-DEV the plan with the highest probability is plan 1 (0.31), 1 (0.28), 4 (0.33), and 4 (0.39) for each of the 25%, 50%, 75% and 100% participation levels. The respective plan with the lowest probability is 3 (0.22), 3 (0.22), 2 (0.20), and 2 (0.17).

Figure 6a illustrates the mean discomfort for MIN-DEV, MIN-COST and control data under varied participation level. A discomfort envelope is defined by the upper and lower bounds when all agents select plan 4 and plan 1 respectively. This is because the slots used are ranked according to the likelihood of usage. Given the plan selections shown in Figure 5, this also explains why MIN-DEV and MIN-COST are positioned closer to the lower bound. MIN-COST has on average 19.6% lower discomfort than MIN-DEV. Moreover, the striking lower discomfort of EPOS compared to controlled data is a result of the plan generation design and the ranking of the slots as well. By taking a careful look in Figure 1, it can be observed that Figure 1b in window 3 has higher discomfort than the plan of Figure 1c with zero discomfort because of the likelihood of utilization during charging. Moreover, the mean discomfort for MIN-COST is on average 0.00187, 0.00147, 0.00161 and 0.00170 for 25%, 50%, 75% and 100% participation level. A similar trend is confirmed for MIN-DEV. This means that a low number of participating agents has to make more disruptive decisions to anticipate for the missing contributions of the non-participating agents. The shift of the selection from plan 4 under 100% participation level towards plan 1 and 2 further justify this finding.

Figure 6b illustrates the fairness for MIN-DEV, MIN-COST and control data under varied participation levels. A fairness envelope is defined by the upper and lower bounds when all agents select plan 1 and plan 4 respectively. Fairness shows the reversed pattern of discomfort. MIN-COST has on average 0.038% higher fairness than MIN-DEV. The mean fairness for MIN-COST is on average 0.9960, 0.9966, 0.9962 and 0.9960 for 25%, 50%, 75% and 100% participation level. A similar trend is confirmed for MIN-DEV.

B. *Future forecasting*

For this analysis, we model the possible future impact of EVs on power infrastructure. As our data is from the state of Californian, we use this state as a case study, where all auxiliary data is respective to this state.

EV Adoption: From numerous statistics, the number of sold EVs is growing yearly (see Figure 7 for Californian sales) with a projected penetration in the automotive market at 22% by 2025 according to various studies [1]. As these vehicles will be sourcing their power from the current and projected infrastructure, it is important to understand how the adoption of EVs will affect the load on the infrastructure. We model and investigate this scenario in this section. For any technological advancement that brings a product to market, there is a well studied notion of adoption by the public –

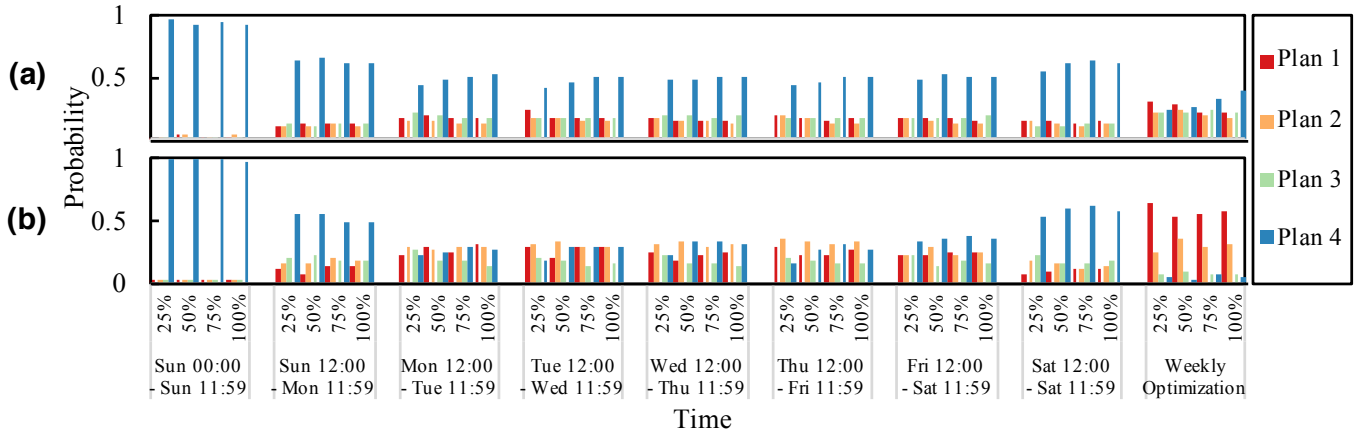

Fig. 5. Plan selections under varied participation level. (a) MIN-DEV, (ii) MIN-COST.

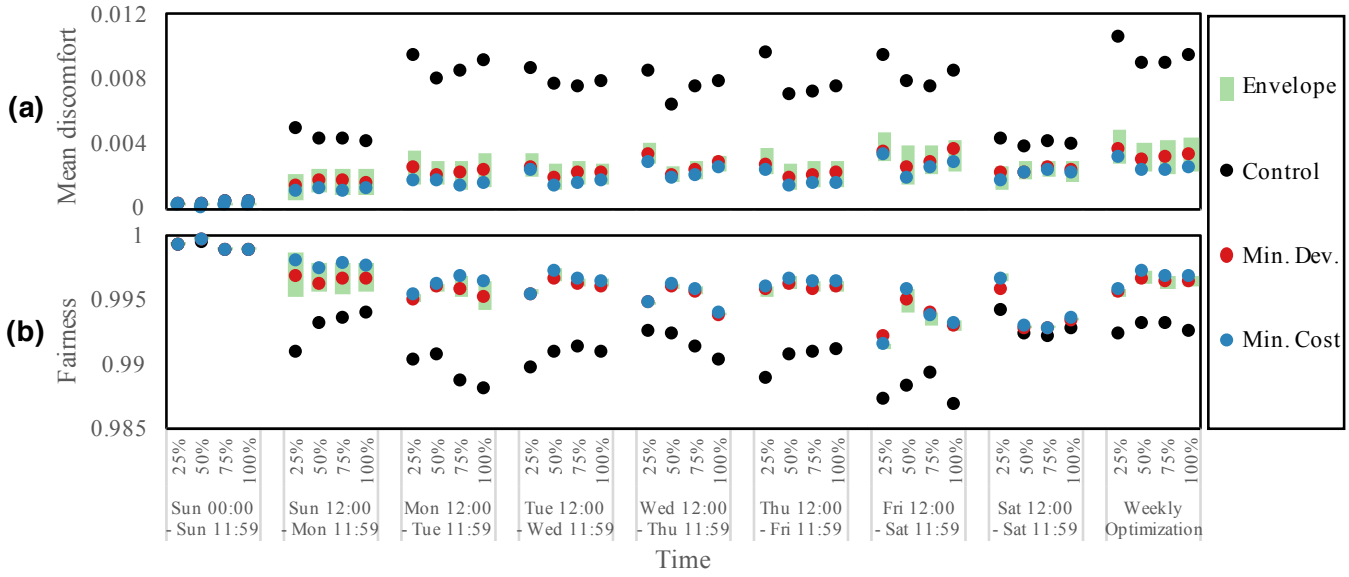

Fig. 6. Discomfort and fairness of MIN-DEV, MIN-COST and control data under varied participation level. The discomfort envelope defines the upper (plan 4) and lower (plan 1) bounds. The fairness envelope defines the upper (plan 1) and lower (plan 4) bounds.

known as the adoption curve [29].[4] The cumulative number of adopters follows a logistic curve, namely

$$S_{\text{EV}}(t) = \frac{C_{EV}}{1 + \exp(-r_A[t_{EV} - t_{\text{mid}}])}, \tag{12}$$

where the cumulative adoption (sales) of EVs as a function of time, $S_{\text{EV}}(t)$, has a market cap, C, whose inflection point is given by t_{mid}, and rapidity of adoption r_A. If we assume that the adoption of EVs follows the same adoption curve, given the current sales data [30], with the future adoption goals given predictions given by the Californian government [31], [32], we model the EV adoption as the dashed line in Figure 7.

From this model of adoption we can assess the impact of future sales on infrastructure.

EV Impact: From our experiments on the pool of 130 EVs discussed above, we investigate a complimentary statistic: the peak power for a given week under different charging paradigms for different EPOS adoption rates. The results are given in Table I.

From these data and the projected sales encompassed by Eq. (12), we can approximate the peak power of the pool of EVs as a function of time:

$$P_{\text{peak}}(t) = \varrho S_{\text{EV}}(t), \tag{13}$$

where ϱ is the average contribution of each EV to the peak power for a given plan. For example, ϱ for the control experiment is given as: $\varrho = 223kW/130EV \approx 1.72kW/EV$. Given Eq. (13) we can therefore forecast the approximate load on the grid due to different charging paradigms and adoption rates, a selection of which is shown in Figure 7b. We note the peak power usage under the Control paradigm performs poorly relative to the other two paradigms. If we are able to incentivize 100% of the EV owners to use the EPOS software, we see that the minimum deviation charging paradigm shows

[4]This assumes that the innovation of EVs spreads amongst the populace via an epidemic-like process.

TABLE I
AGGREGATE POWER USAGE STATISTICS FROM DAILY (D)/ WEEKLY (W) OPTIMIZATION EXPERIMENTS FOR 130 EVS. 'MC' DENOTES MIN. COST EXPERIMENTS, WHEREAS 'MD' DENOTES MINIMUM DEVIATION EXPERIMENTS. ALL POWER VALUES ARE GIVEN IN KILO-WATTS.

Measurement	MC 100%	MD 100%	MC 75%	MD 75%	MC 50%	MD 50%	MC 25%	MD 25%	Control
Peak Power (D)	217.43	119.43	170.83	113.06	145.74	149.75	182.56	181.64	223.00
Peak Power (W)	200.84	121.04	164.50	118.81	141.25	148.34	175.74	184.51	223.00

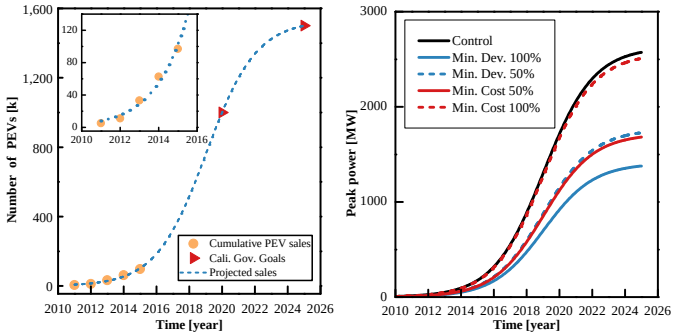

(a) Vehicle Usage **(b)** Driver Profile

Fig. 7. (a) Shown are the cumulative sales of EVs (in 1000s of units) within the state of California from 2011 to 2015 [30], and the mandated sales by 2020, and 2025 for the state (triangular markers) [31][32]. Fitted to these is a sigmodal curve, often assigned to the diffusion of new technologies in a sector (dashed line). The fitted parameters for Eq. (12) are $r_A = 0.653$ years^{-1}, $C = 1.53 \times 10^6$ EVs, $t_{\text{mid}} = 2019$ years. (b) We approximate the peak power on the grid due to EV charging for various scenarios – see text. We see that under both optimisation regimes: min. cost, and min. deviation, the EPOS algorithm performs better than the Control regime in reducing the peak power. As expected, the minimum deviation regime performs the best.

the substantial savings on peak power over time. In 2025, with 1.5 million EVs, the peak power usage could approach 2573 MW, whereas with full EPOS adoption, this will be cut by over 46% to 1378 MW.

V. CONCLUSION AND FUTURE WORK

This paper concludes that a socio-technical Smart Grid optimization is feasible by decentralized charge control of electrical vehicles. This paper introduces a novel operational planning mechanism running locally by a software agent in each EV. The plans generated minimize user discomfort and social fairness by design as shown in the experimental evaluation. Collective decision-making of the executed plans via the decentralized EPOS mechanism contributes to significantly lower power peaks and energy costs. Moreover, as the participation level increases, discomfort decreases concluding that future demand-response programs with enabling technology characteristics such as the ones of EPOS can contribute to public good and create further business opportunities for utility companies and other stakeholders. Moreover, the findings of this paper are used to project and approximate the effect of optimization in a future forecasting scenario with mass adoption of EVs charged from the Smart Grid.

APPENDIX A: BACKGROUND ON THE DATA

Figure 8 and 9 illustrate some background information about the dataset used.

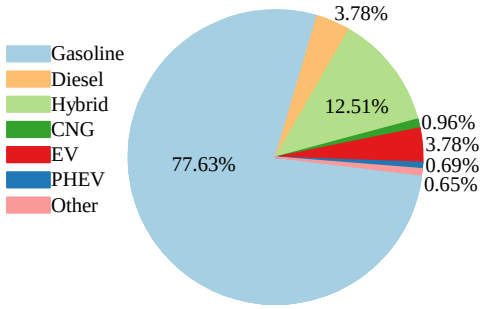

Fig. 8. Vehicles by type contained with the California Household Travel Survey for 2010 - 2012 [23]. EV denotes electric vehicle, and PEH, denotes Plug-in hybrid vehicle.

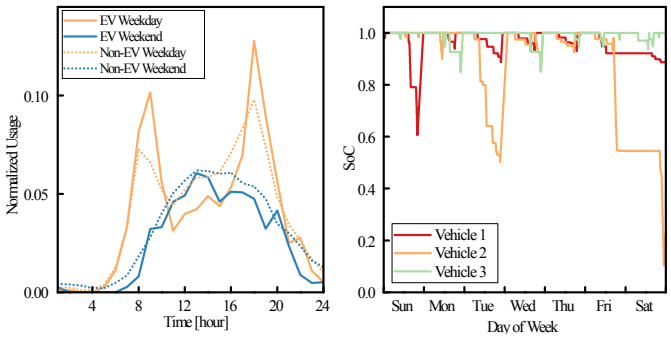

(a) Vehicle Usage **(b)** Driver Profile

Fig. 9. (a) How EVs are used throughout the week – for comparison non-EV usage is also shown. Data for all vehicles are binned within one minute periods, and frequency of 'occupation' of the minute is then divided by the total number of vehicle used. One notes the characteristic peaks during rush hours during the week, usage during the day and the intuitive daytime usage during the weekend days. The qualitative shape of the curves remains the same between the vehicle types (EV and non-EV). We pool both EVs and PHEVs from the data into the category 'EV' shown in this plot. (b) Three SoC profiles for different vehicles (all the same vehicle model – Tesla S [33]) over a period of one week.

APPENDIX B: POWER CONSUMPTION

Figure 10 illustrates the demand curves of the EVs under daily and weekly optimization with MIN-DEV and MIN-COST.

ACKNOWLEDGMENT

REFERENCES

[1] The Goldman Sachs Group, Inc., "The Low Carbon Economy: GS SUSTAIN equity investors guide to a low carbon world, 2015-25," access Date: 2016-07-28. [Online]. Available: http://www.goldmansachs.com/our-thinking/pages/new-energy-landscape-folder/report-the-low-carbon-economy/report.pdf

[2] K. M. Tan, V. K. Ramachandaramurthy, and J. Y. Yong, "Integration of electric vehicles in smart grid: A review on vehicle to grid technologies and optimization techniques," *Renewable and Sustainable Energy Reviews*, vol. 53, pp. 720–732, 2016.

TABLE II
DESCRIPTIVE STATISTICS OF EV MODELS. MPG DENOTES MILES PER GALLON OF GASOLINE.

Model	MPG City/Highway	Battery Cap. (kWh)	Charge Rate (kW)
Nissan Leaf [34]	126/101	24	6.6
Tesla Model S (85 kWh version) [35]	88/90	85	9.6
BMW i3 [36]	137/111	22	7.4
Fiat 500e[37]	121/103	24	6.6
Ford Focus Electric [38]	110/99	23	6.6

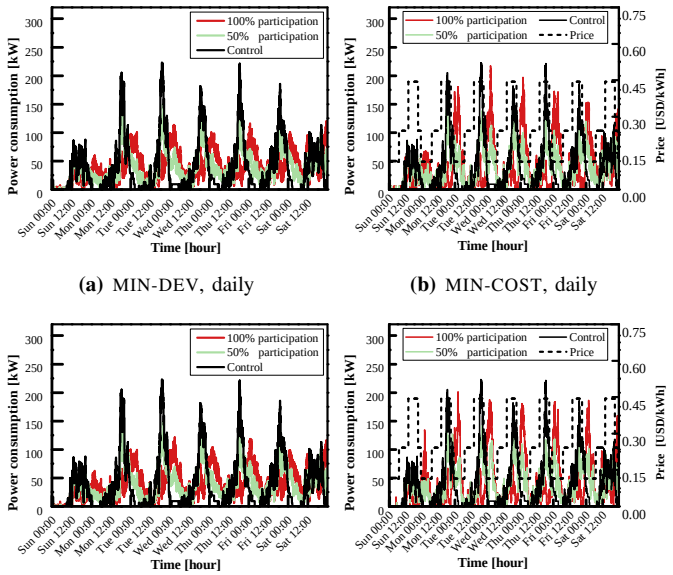

(a) MIN-DEV, daily **(b)** MIN-COST, daily

(c) MIN-DEV, weekly **(d)** MIN-COST, weekly

Fig. 10. Demand curves of the EVs under daily and weekly optimization with MIN-DEV and MIN-COST.

[3] R. C. Green, L. Wang, and M. Alam, "The impact of plug-in hybrid electric vehicles on distribution networks: A review and outlook," *Renewable and Sustainable Energy Reviews*, vol. 15, no. 1, pp. 544–553, 2011.

[4] W. Kempton and J. Tomić, "Vehicle-to-grid power implementation: From stabilizing the grid to supporting large-scale renewable energy," *Journal of power sources*, vol. 144, no. 1, pp. 280–294, 2005.

[5] S. Bahrami and M. Parniani, "Game theoretic based charging strategy for plug-in hybrid electric vehicles," *IEEE Transactions on Smart Grid*, vol. 5, no. 5, pp. 2368–2375, 2014.

[6] E. Pournaras, M. Warnier, and F. M. Brazier, "Local agent-based self-stabilisation in global resource utilisation," *International Journal of Autonomic Computing*, vol. 1, no. 4, pp. 350–373, 2010.

[7] C.-K. Wen, J.-C. Chen, J.-H. Teng, and P. Ting, "Decentralized plug-in electric vehicle charging selection algorithm in power systems," *IEEE Transactions on Smart Grid*, vol. 3, no. 4, pp. 1779–1789, 2012.

[8] H.-M. Chung, B. Alinia, N. Crespi, and C.-K. Wen, "An ev charging scheduling mechanism to maximize user convenience and cost efficiency," *arXiv preprint arXiv:1606.00998*, 2016.

[9] M. Georgeff, "Communication and interaction in multi-agent planning," *Readings in distributed artificial intelligence*, vol. 313, pp. 125–129, 1988.

[10] M. De Weerdt, A. Ter Mors, and C. Witteveen, "Multi-agent planning: An introduction to planning and coordination," in *In: Handouts of the European Agent Summer*. Citeseer, 2005.

[11] K. Konolige and N. J. Nilsson, "Multiple-agent planning systems," in *AAAI*, vol. 80, 1980, pp. 138–142.

[12] M. Barbati, G. Bruno, and A. Genovese, "Applications of agent-based models for optimization problems: A literature review," *Expert Systems with Applications*, vol. 39, no. 5, pp. 6020–6028, 2012.

[13] E. Pournaras, "Multi-level reconfigurable self-organization in overlay services," Ph.D. dissertation, TU Delft, Delft University of Technology, 2013.

[14] E. Pournaras, M. Vasirani, R. E. Kooij, and K. Aberer, "Decentralized planning of energy demand for the management of robustness and discomfort," *IEEE Transactions on Industrial Informatics*, vol. 10, no. 4, pp. 2280–2289, 2014.

[15] ——, "Measuring and controlling unfairness in decentralized planning of energy demand," in *Energy Conference (ENERGYCON), 2014 IEEE International*. IEEE, 2014, pp. 1255–1262.

[16] (2016) Power consumption of nissan model. Last accessed: July 2016. [Online]. Available: http://www.nissanusa.com/electric-cars/leaf/versions-specs/version.s.html

[17] W. Sierzchula, S. Bakker, K. Maat, and B. van Wee, "The competitive environment of electric vehicles: An analysis of prototype and production models," *Environmental Innovation and Societal Transitions*, vol. 2, pp. 49 – 65, 2012.

[18] S. Lacroix, M. Hilairet, and E. Laboure, "Design of a battery-charger controller for electric vehicle based on rst controller," in *2011 IEEE Vehicle Power and Propulsion Conference*, Sept 2011, pp. 1–6.

[19] E. Pournaras, M. Yao, R. Ambrosio, and M. Warnier, "Organizational control reconfigurations for a robust smart power grid," in *Internet of Things and Inter-cooperative Computational Technologies for Collective Intelligence*. Springer, 2013, pp. 189–206.

[20] P. Gas and E. Company, "Electric schedule ev, residential time-of-use service for plug-in electric vehicle customers," 2016, data was accessed: 2016-07-26. [Online]. Available: http://www.pge.com/tariffs/tm2/pdf/ELEC_SCHEDS_EV.pdf

[21] J. Shen, S. Dusmez, and A. Khaligh, "Optimization of sizing and battery cycle life in battery ultracapacitor hybrid energy storage systems for electric vehicle applications," *IEEE Transactions on Industrial Informatics*, vol. 10, no. 4, pp. 2112–2121, 2014.

[22] E. Pournaras, M. Warnier, and F. M. Brazier, "Adaptive self-organization in distributed tree topologies," *International Journal of Distributed Systems and Technologies (IJDST)*, vol. 5, no. 3, pp. 24–57, 2014.

[23] N. R. E. Laboratory, "Transportation secure data center," 2015, date TSDC data was accessed: 2016-07-18. [Online]. Available: www.nrel.gov/tsdc

[24] J. Liu, "Analysis of EV Charging Load Based on Household Driving Data in California," Master's thesis, University of California Riverside, 12 2015.

[25] O. o. E. E. U.S. Department of Energy and R. Energy, "The title of the work," 2000, access Date: 2016-07-27. [Online]. Available: https://www.gpo.gov/fdsys/pkg/FR-2000-06-12/pdf/00-14446.pdf

[26] When conducting experiments with vehicle market share, we assign each vehicle at random, a model, such that number of vehicles for each model, matches that of the market share. If the vehicle is assigned a model, and it's weekly driving profile exceeds the battery capacity (see Table II for such information), it is assigned a model that can accomplish this profile.

[27] As some inconsistency across various sales data sources are found, the most confident available source will be used. The confidence level from highest to lowest are manufacturer sales reports, U.S. Clean Vehicle Rebate Project (CVRP) and U.S. DOE Alternative Fuels Data Center (AFDC) sourced from hybridcar.com. U.S. Sales of Nissan Leaf and BMW i3 are available in manufacturer websites. For Tesla Model S only data 2014-15 are available from manufacturer. Fiat 500e sales is obtained from U.S. CVRP. All the rest of data are obtained from U.S. DOE AFDC.

[28] W. Galuba, K. Aberer, Z. Despotovic, and W. Kellerer, "Protopeer: Distributed systems prototyping toolkit," in *2009 IEEE Ninth International Conference on Peer-to-Peer Computing*, Sept 2009, pp. 97–98.

[29] H. P. Young, "Innovation diffusion in heterogeneous populations: Contagion, social influence, and social learning," *The American economic review*, pp. 1899–1924, 2009.

[30] C. N. C. D. Association, "California Auto Outlook 4th Quarter 2015, 2016 February. Volume 12, Number 1, Page 1," 2016, Date accessed: 2016-07-21. [Online]. Available: http://www.cncda.org/Auto_Outlook.asp

[31] C. E. Commission, "Tracking process: Plug-in electric vehicles," 2015, date accessed: 2016-07-18. [Online]. Available: http://www.energy.ca.gov/renewables/tracking_progress/documents/electric_vehicle.pdf

[32] Californian Governer's office of Planning and Research, "Governors Interagency Working Group on Zero-Emission Vehicles 2013 ZEV Action Plan: An Roadmap toward 1.5 Million Zero-Emission Vehicles on California Roadways by 2025," 2013, data was accessed: 2016-07-19. [Online]. Available: https://www.opr.ca.gov/docs/Governors_Office_ZEV_Action_Plan_(02-13).pdf

[33] T. Motors, "Telsa model s information," 2016, data was accessed: 2016-07-20. [Online]. Available: https://www.tesla.com/models
[34] N. M. Company, "Nissan leaf specification," 2016, data was accessed: 2016-07-26. [Online]. Available: http://www.nissanusa.com/electric-cars/leaf/versions-specs/
[35] T. Motor, "Tesla model s and charging specification," 2015, data was accessed: 2015-10-01. [Online]. Available: https://www.tesla.com/models
[36] B. M. W. AG, "Bmw i3 specification," 2016, data was accessed: 2016-07-26. [Online]. Available: http://www.bmwusa.com/Standard/Content/Vehicles/2016/i3/BMWi3/Features_and_Specs/
[37] F. Automobiles, "Fiat 500e features," 2016, data was accessed: 2016-07-26. [Online]. Available: http://www.fiatusa.com/en/2016/500e/
[38] F. M. Company, "Ford electric focus features," 2016, data was accessed: 2016-07-26. [Online]. Available: http://www.ford.com/cars/focus/trim/electric/